Chromospheric line diagnostics capability I

Carlos Quintero Noda

ISAS/JAXA ITYF fellow

February 26 – 28th, 2018
DKIST CSP Workshop in Nagoya

Chromospheric line diagnostics capability I

Introduction

Aims

- We plan to compare well-known chromospheric lines
- We examine their polarimetric capabilities for future observations

Method

- We first revise the literature, mainly recent observations
- Then, we expand our knowledge with theoretical studies
- This is the first step towards a guide/manual for future observations

Chromospheric line diagnostics capability I

Na I D_1 & D_2 lines

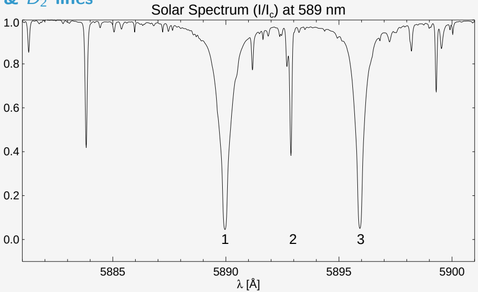

- Very deep and narrow lines (**labels 1 and 3**) that reach higher than $\sim$ 800 km
- No solar blends or telluric lines
- Low Landé factor but very sensitive to the scattering polarization (e.g., Stenflo 2000)

Chromospheric line diagnostics capability I

Na I D_1 & D_2 lines

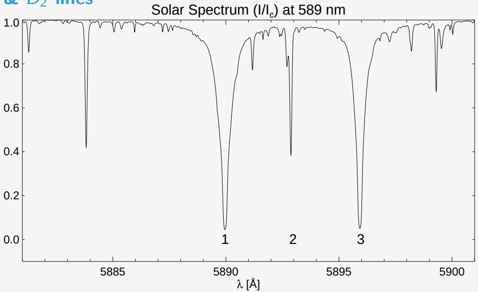

- Very deep and narrow lines (**labels 1 and 3**) that reach higher than $\sim$ 800 km
- No solar blends or telluric lines
- Low Landé factor but very sensitive to the scattering polarization (e.g., Stenflo 2000)

Recent works: Jess et al. (2010)

- Magnetic bright points
- Na I D_1 core shows strong downflows on MBPs
- In addition to co-spatial underlying magnetic field concentrations

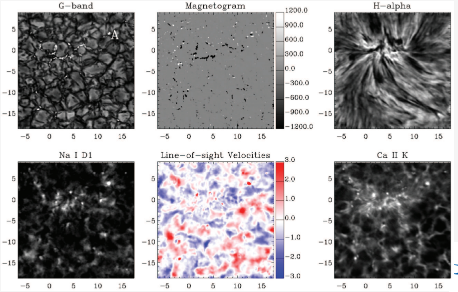

Chromospheric line diagnostics capability I

Na I D_1 & D_2 lines

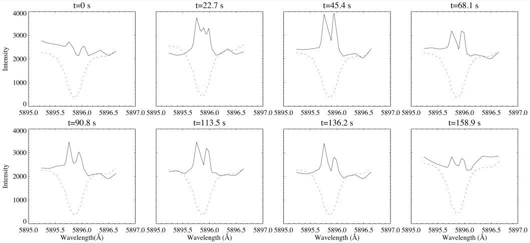

Recent works: Kuridze et al. (2016)

- M flare observations
- Intensity profiles in emission!
- Profile asymmetries are produced by velocity gradients in the lower solar atmosphere

Chromospheric line diagnostics capability I

Na I D_1 & D_2 lines

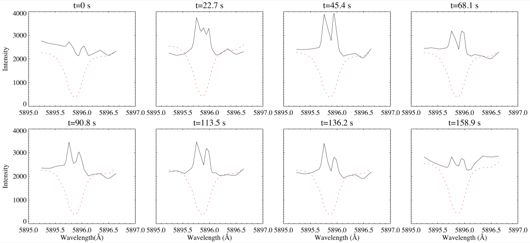

Recent works: Kuridze et al. (2016)

- M flare observations
- Intensity profiles in emission!
- Profile asymmetries are produced by velocity gradients in the lower solar atmosphere

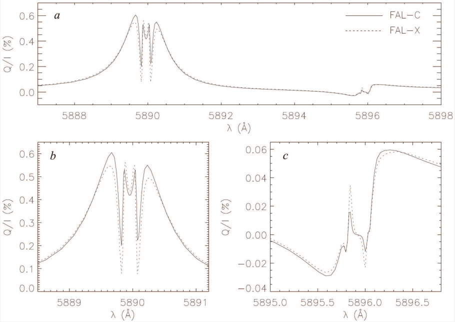

Recent works: Belluzzi et al. (2015)

- Enigmatic scattering polarization on Na I D_1
- Reproduced after taking into account the spectral structure of the anisotropic radiation responsible for the optical pumping
- NOTE: Na I D_2 produces large scattering signals!

Chromospheric line diagnostics capability I

Mg I *b* lines

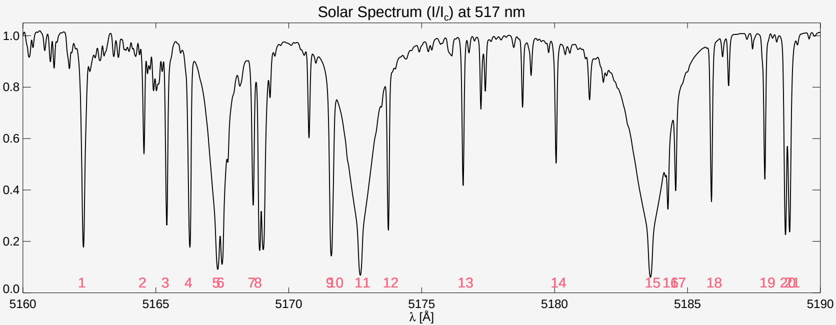

- Mg I *b* lines are labelled as **5, 11, and 15**. The most capable for polarimetry is Mg I b_2, i.e. label 11 (see Appendix)
- Very deep and wide lines that reach higher than $\sim$ 800 km.
- Moderate Landé factor (i.e. g_{eff}=1.75) but very broad line

Chromospheric line diagnostics capability I

Mg I *b* lines

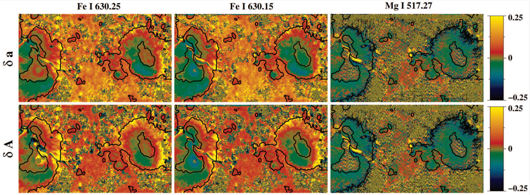

Recent works: Deng et al. (2010)

- Results indicate that Mg I forms around or just above the temperature minimum region
- The outer penumbrae and pores show similar Stokes *V* asymmetry behaviour that changes from positive values in the photosphere to negative values in the low chromosphere
- Discrepancies due to the three-dimensional structure of the magnetic and velocity fields

Chromospheric line diagnostics capability I

Mg I *b* lines

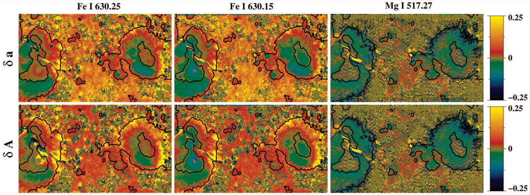

Recent works: Deng et al. (2010)

- Results indicate that Mg I forms around or just above the temperature minimum region
- The outer penumbrae and pores show similar Stokes *V* asymmetry behaviour that changes from positive values in the photosphere to negative values in the low chromosphere
- Discrepancies due to the three-dimensional structure of the magnetic and velocity fields

Recent works: Rutten et al. (2015)

- Ellerman bombs are transient brightenings of the wings of the solar Balmer lines
- They found a diffuse brightness in Mg I and Na I too
- A possible explanation: a post-bomb hot-cloud phenomenon

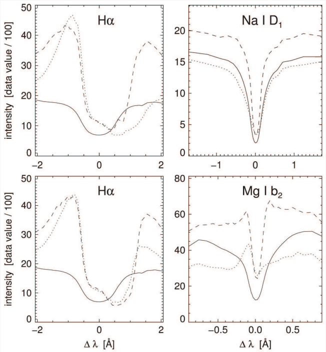

Chromospheric line diagnostics capability I

Ca II IR lines

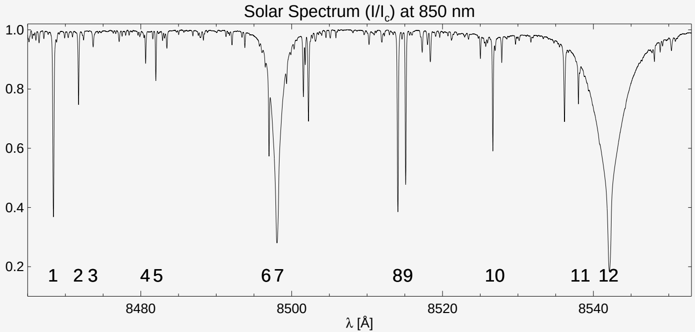

- Ca II IR triplet is very famous, together with He I 10830, for polarimetry
- Ca II 8542 (**label 12**) is very deep and reaches higher than $\sim$ 1000 km
- Very sensitive to B photospheric lines nearby (**labels 1 and 8**)
- Recent works
  - Sunspot Chromosphere (Rouppe van der Voort et al. 2010, de la Cruz Rodríguez et al. 2013)
  - Disk counterpart of spicules (Langangen et al. 2008, Sekse et al. 2011, Rouppe van der Voort et al. 2015)
  - Quiet Sun chromosphere (Vecchio et al. 2009, Cauzzi et al. 2009a,b)

Chromospheric line diagnostics capability I

Ca II IR lines

Recent works: de la Cruz Rodríguez et al. (2013)

- Umbral flashes (UFs) are brightenings observed in the chromospheric core of the Ca II lines
- UFs have very fine structure with hot and cool material intermixed at sub-arc sec scales
- The shock front is roughly 1000 K hotter than the surrounding material

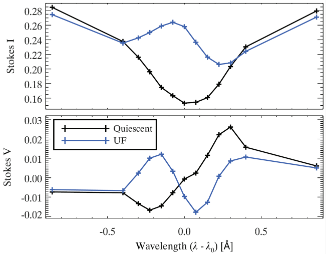

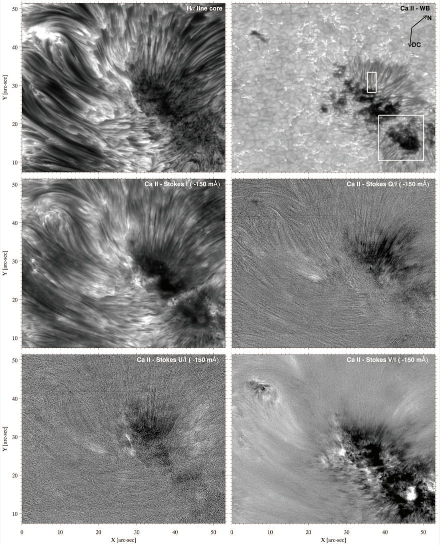

Chromospheric line diagnostics capability I

K I D_1 & D_2 lines

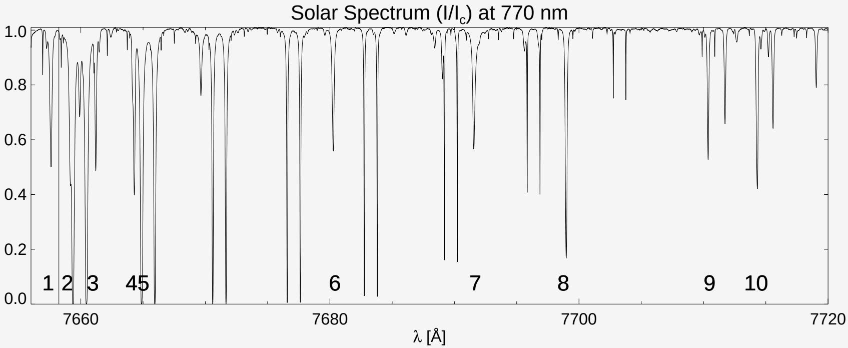

- K I D lines are similar to the Na I lines, narrow and deep spectral lines
- They reach lower heights, around $\sim$ 600 km and K I D_2 is blocked by telluric O_2 while K I D_1 (**label 8**) is accessible from the ground
- Low Landé factor but very sensitive to the LOS velocity at around T_{min}
- Vastly used for helio-seismology in the 80s and 90s (e.g., Claverie et al. 1982)

Chromospheric line diagnostics capability I

Comparison between spectral lines I. Observations

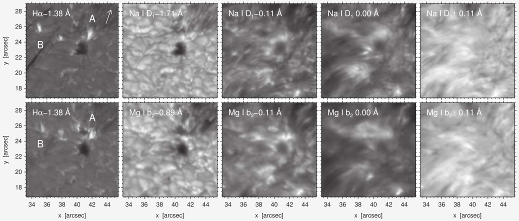

- Rutten et al. (2010, 2015) compare the Na I and Mg I lines
- They seem to form at similar heights
- Maybe observing just one is enough

Chromospheric line diagnostics capability I

Comparison between spectral lines I. Observations

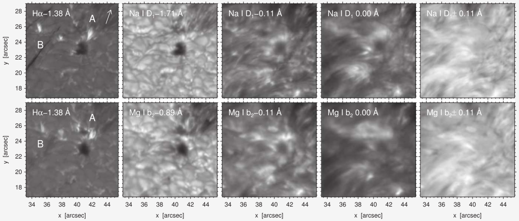

- Rutten et al. (2010, 2015) compare the Na I and Mg I lines
- They seem to form at similar heights
- Maybe observing just one is enough

- Cauzzi et al. 2009a,b compare the Ca II 8542 Å line with H_α
  - See also slide 7 (de la Cruz Rodríguez et al. (2013)
- Fibrils are more conspicuous on H_α
- However, we can infer $\vec{B}$ with Ca II
  - See H_α Response Function to $\vec{B}$ in Socas Navarro & Uitenbroek (2004)

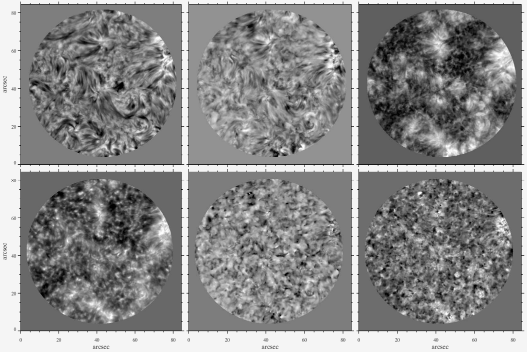

Chromospheric line diagnostics capability I

Comparison between spectral lines II. Theoretical studies

- We employ a single code for solving the RTE
  - RH (Uitenbroek 2001, 2003)
- The four Stokes parameters are computed
- NLTE, CRD and only Zeeman effect

- 1D semi-empirical model
  - FALC (Fontenla et al. 1993)
- 3D MHD simulations
  - Bifrost enhanced network (Carlsson et al. 2016)

Chromospheric line diagnostics capability I

Comparison between spectral lines II. Theoretical studies

- We employ a single code for solving the RTE
  - RH (Uitenbroek 2001, 2003)
- The four Stokes parameters are computed
- NLTE, CRD and only Zeeman effect
- 1D semi-empirical model
  - FALC (Fontenla et al. 1993)
- 3D MHD simulations
  - Bifrost enhanced network (Carlsson et al. 2016)

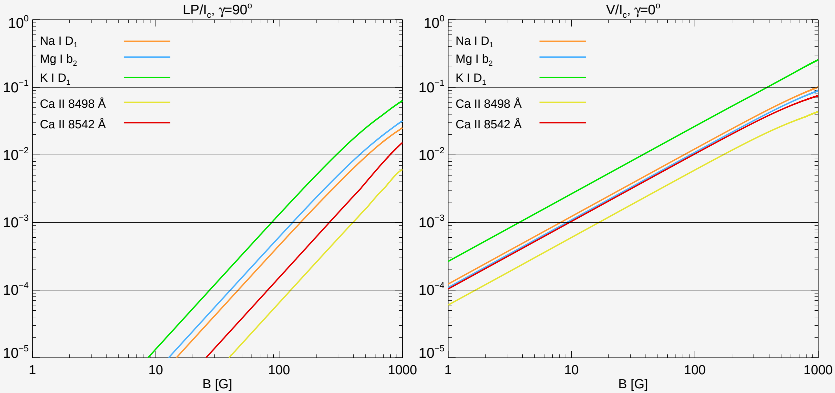

Chromospheric line diagnostics capability I

1D Response Functions using the FALC model and $B = 1000$ G, $\gamma = 45^\circ$, $\phi = 45^\circ$

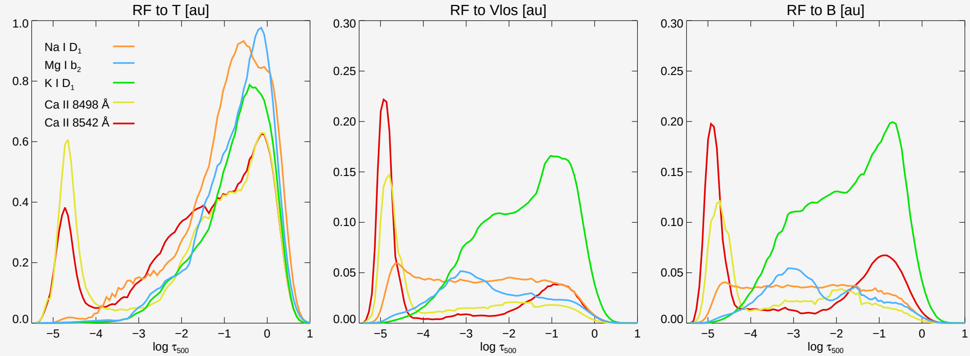

- Ca II lines are sensitive to T at all heights
- K I and Mg I only at low heights
- K I very sensitive to velocity at middle heights
- Ca II lines are very sensitive to B in the chromosphere
  - K I at much lower layers
- Mg I and Na I in between K I and Ca II

Chromospheric line diagnostics capability I

Bifrost enhanced simulation

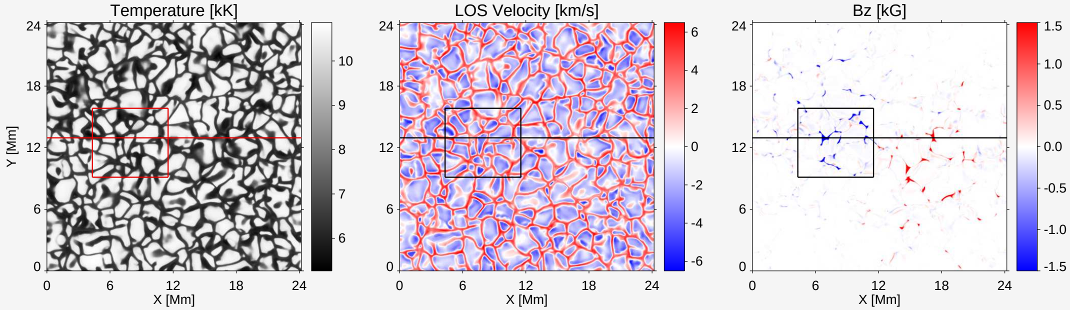

Snapshot 385 of the enhanced network simulation (Carlsson et al. 2016). Horizontal line represents the slice used for comparing the height of formation while the square represents the region used for examining the polarization signals.

Chromospheric line diagnostics capability I

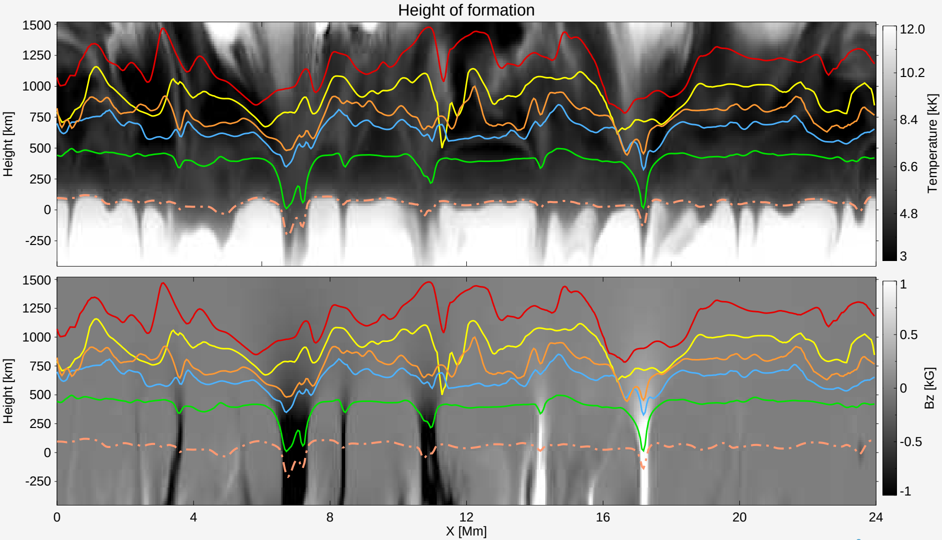

Height where τ=1 for the line core of Na I D_1 (orange), Mg I b_2 (blue), K I D_1 (green), Ca II 8498 Å (yellow), and 8542 Å (red). Dashed orange to τ=1 at continuum wavelengths.

Chromospheric line diagnostics capability I

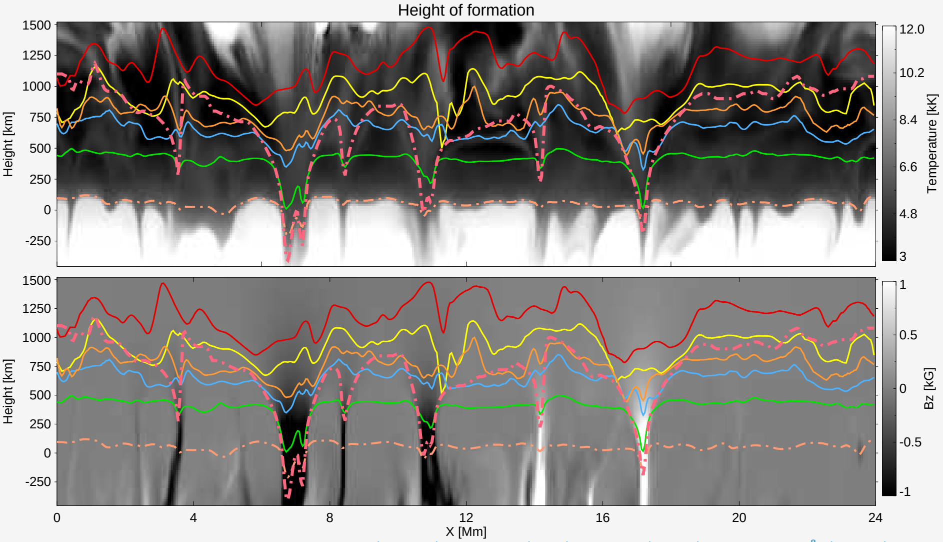

Height where τ=1 for the line core of Na I D_1 (orange), Mg I b_2 (blue), K I D_1 (green), Ca II 8498 Å (yellow), and 8542 Å (red). Dashed pink corresponds to $\beta \sim 1$ and dashed orange to τ=1 at continuum wavelengths.

Chromospheric line diagnostics capability I

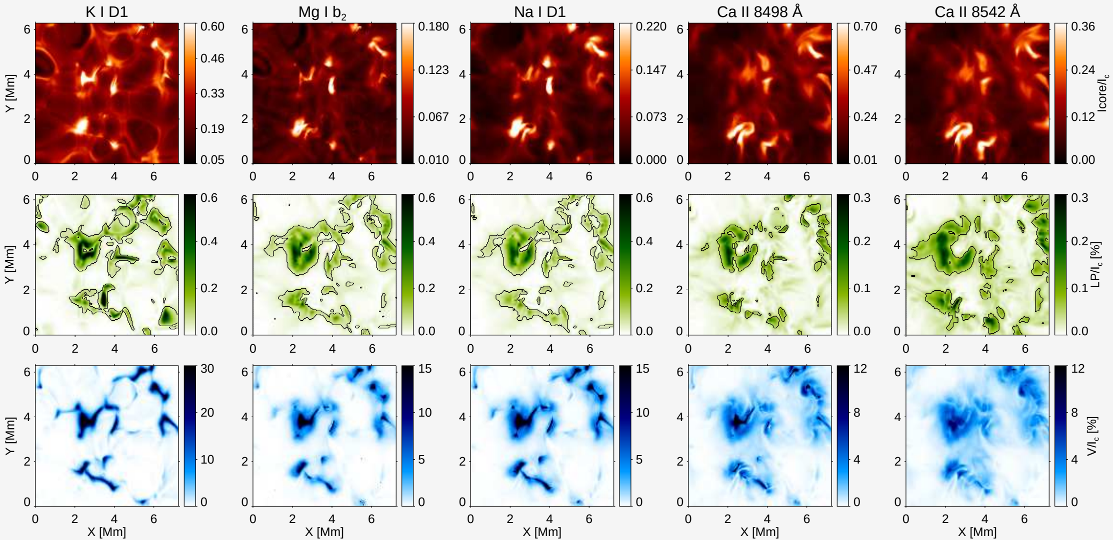

Line core intensity (up), total LP (middle), and CP (bottom) for selected chromospheric lines. The FOV corresponds to the highlighted square in slide 12. Contours represent LP$> 5 \times 10^{-4}$ of I_c

Chromospheric polarimetry

- The most complete chromospheric line is Ca II 8542 Å

Chromospheric polarimetry

- The most complete chromospheric line is Ca II 8542 Å
- However, we recommend observing additional lines to increase the height coverage
  - Upper photosphere: K I D_1
    - It forms slightly higher than photospheric lines
    - Pol. signals are larger than the rest of chromospheric lines

Chromospheric polarimetry

- The most complete chromospheric line is Ca II 8542 Å
- However, we recommend observing additional lines to increase the height coverage
  - Upper photosphere: K I D_1
    - It forms slightly higher than photospheric lines
    - Pol. signals are larger than the rest of chromospheric lines
  - Low chromosphere: Na I or Mg I (the former seems more adequate)
    - Forms higher and **very** sensitive to scattering polarization

Chromospheric polarimetry

- The most complete chromospheric line is Ca II 8542 Å
- However, we recommend observing additional lines to increase the height coverage
  - Upper photosphere: K I D_1
    - It forms slightly higher than photospheric lines
    - Pol. signals are larger than the rest of chromospheric lines
  - Low chromosphere: Na I or Mg I (the former seems more adequate)
    - Forms higher and **very** sensitive to scattering polarization
  - Middle chromosphere: Ca II 8498 Å (it forms a bit lower than 8542 Å)

Chromospheric polarimetry

- The most complete chromospheric line is Ca II 8542 Å
- However, we recommend observing additional lines to increase the height coverage
  - Upper photosphere: K I D_1
    - It forms slightly higher than photospheric lines
    - Pol. signals are larger than the rest of chromospheric lines
  - Low chromosphere: Na I or Mg I (the former seems more adequate)
    - Forms higher and **very** sensitive to scattering polarization
  - Middle chromosphere: Ca II 8498 Å (it forms a bit lower than 8542 Å)

Finally, all the studies shown here do not include any instrumental degradation. Thus, in order to perform chromospheric polarimetry, we should nominally work with a noise level lower than 5×10^{-4} of I_c

Thanks!

Contact information

Name: Carlos Quintero Noda
Position: ITYF at ISAS/JAXA
e-mail: carlos@solar.isas.jaxa.jp

Related publications: Quintero Noda et al. (2016, 2017a,b,c, 2018)

Chromospheric line diagnostics capability I

Appendix: Spectral lines at 589 nm

	Atom	λ [Å]	$\log gf$	L_l	U_l	$\bar{g}$
1	Na I (D_2)	5889.95	0.101	$^2S_{1/2}$	$^2P^0_{3/2}$	1.167
2	Ni I	5892.88	-2.340	$^3P_0$	$^1P^0_1$	1.000
3	Na I (D_1)	5895.59	-0.184	$^2S_{1/2}$	$^2P^0_{1/2}$	1.333

Table: Spectral lines included in the 589 nm window presented in slide 2. Each column, from left to right, contains the number assigned to each line, the corresponding atomic species, line core wavelength, $\log gf$ of the transition, and the spectroscopic notation of the lower and the upper level (retrieved from the database of R. Kurucz, Kurucz et al. 1995). The last column contains the effective Landé factor computed assuming L-S coupling.

Chromospheric line diagnostics capability I

Appendix: Spectral lines at 517 nm

	Atom	λ [Å]	log gf	L_l	U_l	$\bar{g}$
1	Fe I	5162.27	0.020	$^5F^0_5$	$^5F_5$	1.40
2	Fe I	5164.55	-1.360	$^3G^0_4$	$^3F_3$	1.00
3	Fe I	5165.41	-0.026	$^5F^0_4$	$^5F_4$	1.35
4	Fe I	5166.28	-4.195	$^5D_4$	$^7D^0_5$	1.80
5	Mg I	5167.32	-0.870	$^3P^0_0$	$^3S_1$	2.00
6	Fe I	5167.48	-1.260	$^3F_4$	$^3D^0_3$	1.13
7	Ni I	5168.65	-0.430	$^5F^0_3$	$^3G_4$	0.75
8	Fe I	5168.89	-3.969	$^5D_3$	$^7D^0_3$	1.50
9	Fe I	5171.60	-1.793	$^3F_4$	$^3F^0_4$	1.25
10	Fe I	5171.67	-1.912	$^3D_3$	$^1G^0_4$	0.50
11	Mg I	5172.68	-0.393	$^3P^0_1$	$^3S_1$	1.75
12	Ti I	5173.74	-1.118	$^3F_2$	$^3F^0_2$	0.67
13	Ni I	5176.55	-0.440	$^1D^0_2$	$^1D_2$	1.00
14	Fe I	5180.06	-1.260	$^3G^0_3$	$^3F_2$	0.83
15	Mg I	5183.60	-0.171	$^3P^0_2$	$^3S_1$	1.25
16	Fe I	5184.27	-1.000	$^5F^0_2$	$^5F_3$	1.50
17	Ni I	5184.56	-0.833	$^3D^0_2$	$^3P_1$	1.00
18	Ti II	5185.91	-1.350	$^2G_{7/2}$	$^2G^0_{7/2}$	0.89
19	Fe I	5187.92	-1.260	$^3F_3$	$^3D^0_2$	1.00
20	Ti II	5188.68	-1.260	$^2D_{5/2}$	$^2D^0_{5/2}$	1.25
21	Ca I	5188.84	-0.090	$^1P^0_1$	$^1D_2$	1.00

Table: Spectral lines included in the 517 nm window presented in slide 4. Each column, from left to right, contains the number assigned to each line, the corresponding atomic species, line core wavelength, log gf of the transition, and the spectroscopic notation of the lower and the upper level (retrieved from the database of R. Kurucz, Kurucz et al. 1995). The last column contains the effective Landé factor computed assuming L-S coupling.

Chromospheric line diagnostics capability I

Appendix: Spectral lines at 850 nm

	Atom	λ [Å]	log gf	L_l	U_l	g_{eff}	I_{core} [au]
1	Fe I	8468.41	-2.072	$^5P_1$	$^5P_1^0$	2.50	3649
2	Fe I	8471.74	-0.915	$^5D_3^0$	$^5D_3$	1.50	7510
3	Mg I	8473.69	-2.020	$^3P_2^0$	$^3S_1$	1.25	9347
4	Fe I	8480.63	-1.685	$^5D_2^0$	$^5P_1$	1.00	8784
5	Fe I	8481.98	-1.647	$^3F_2$	$^3D_1^0$	0.75	8230
6	Fe I	8496.99	-0.821	$^3F_3^0$	$^3F_2$	1.50	5831
7	Ca II	8498.02	-1.318	$^2D_{3/2}$	$^2P_{3/2}$	1.07	2856
8	Fe I	8514.07	-2.229	$^5P_2$	$^5P_2^0$	1.83	3840
9	Fe I	8515.11	-2.073	$^3G_3$	$^3G_3^0$	0.75	4734
10	Fe I	8526.67	-0.760	$^5D_4^0$	$^5D_4$	1.50	5858
11	Fe I	8538.01	-2.446	$^5D_4^0$	$^7G_4$	1.40	7423
12	Ca II	8542.09	-0.360	$^2D_{5/2}$	$^2P_{3/2}^0$	1.10	1823

Table: Spectral lines included in the infrared 850 nm window. Each column, from left to right contains the number we assigned to each line in slide 6, the corresponding atomic species, line core wavelength centre, the oscillator strength of the transition, the spectroscopic notation of the lower and the upper level, the effective Landé factor, and the line core intensity in arbitrary units (the continuum level corresponds to 10000).

Chromospheric line diagnostics capability I

Appendix: Spectral lines at 770 nm

	Atom	λ [Å]	log gf	L_l	U_l	g_{eff}	I_{core} [au]
1	Mg I	7657.60	-1.120	$^3S_1$	$^3P^0_2$	1.25	4917
2	Mg I	7659.15	-1.340	$^3S_1$	$^3P^0_1$	1.75	6736
3	Fe I	7661.20	-0.914	$^5F^0_3$	$^5F_4$	1.50	4791
4	Fe I	7664.30	-1.682	$^3G_4$	$^3F^0_3$	1.00	3941
5	K I	7664.90	0.1345	$^2S_{1/2}$	$^2P^0_{3/2}$	1.16	——
6	Si I	7680.25	-0.690	$^1P_1$	$^1D^0_2$	1.00	5488
7	Mg I	7691.55	-0.800	$^1D_2$	$^1F^0_3$	1.00	5568
8	K I	7698.97	-0.169	$^2S_{1/2}$	$^2P^0_{1/2}$	1.33	1663
9	Fe I	7710.36	-1.113	$^5F^0_4$	$^5F_5$	1.50	5152
10	Ni I	7714.32	-2.200	$^3P_2$	$^3P^0_2$	1.50	4132

Table: Spectral lines included in the infrared 770 nm window. Each column, from left to right, contains the number assigned to each line (see slide 8), the corresponding atomic species, line core wavelength, log gf of the transition, the spectroscopic notation of the lower and the upper level, the effective Landé factor, and the line core intensity in arbitrary units (the continuum level corresponds to 10000).

Chromospheric line diagnostics capability I

Appendix: Spectrum at 517 nm

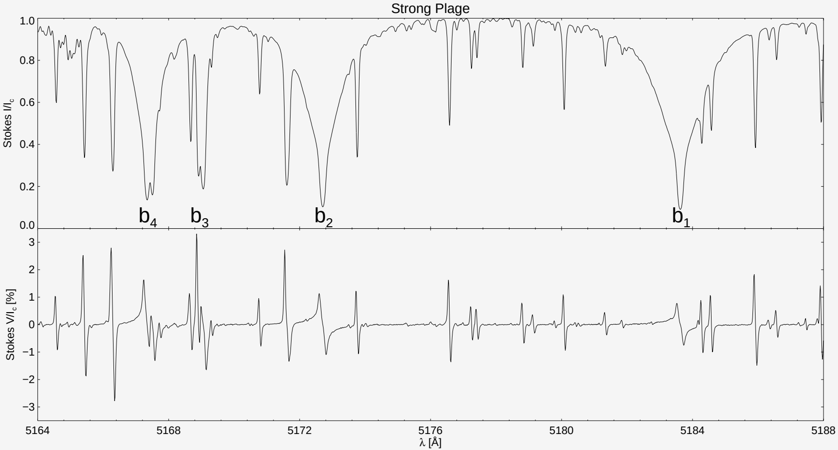

Figure: Solar spectrum from a strong plage region observed in 1979 and presented in Stenflo et al. (1984) for the first time. Top panel shows the intensity while bottom panel displays the circular polarization signals, both normalized to the continuum intensity (I_c). The data for this analysis have been provided in electronic form by IRSOL as a compilation by Stenflo et al. (2014).